Journal of Traditional and Complementary Medicine 14 (2024) 300–311

Contents lists available at ScienceDirect

Journal of Traditional and Complementary Medicine

journal homepage: www.elsevier.com/locate/jtcme

Nootropic effect of Indian Royal Jelly against okadaic acid induced rat model of Alzheimer's disease: Inhibition of neuroinflammation and acetylcholineesterase

Rahul Dubey [a,b], L. Sathiyanarayanan [a,*], Sandeep Sankaran [c], S. Arulmozhi [d]

[a] Department of Pharmaceutical Chemistry, Poona College of Pharmacy, Bharati Vidyapeeth (Deemed to be University), Pune, Maharashtra, India
[b] Department of Pharmacy, Government Polytechnic, Ratnagiri, Maharashtra, India
[c] Department of Quality Assurance Techniques, Poona College of Pharmacy, Bharati Vidyapeeth (Deemed to be University), Pune, Maharashtra, India
[d] Department of Pharmacology, Poona College of Pharmacy, Bharati Vidyapeeth (Deemed to be University), Pune, Maharashtra, India

ARTICLE INFO

Keywords:
Indian royal jelly
Alzheimer's disease
10-Hydroxy-2-decenoic acid
Okadaic acid
Tau protein kinases
Neuroinflammation

ABSTRACT

Background: Royal jelly is an anti-inflammatory, antioxidant, and neuroprotective bee product. There are several sources for royal jelly and one of them is Indian Royal Jelly (IRJ). However, the neuroprotective actions of IRJ and the underlying molecular mechanisms involved are not well known.

Objective: To evaluate the neuroprotective effect of IRJ in the okadaic acid (OKA)-induced Alzheimer's disease (AD) model in rats.

Methods: In male Wistar rats, OKA was intracerebroventricularly (ICV) administered, and from day 7, they were treated orally with IRJ or memantine for 21 days. Spatial and recognition learning and memory were evaluated from days 27–34; employing the Morris water maze (MWM) and the novel object recognition tests (NORT), respectively. *In vitro* biochemical measurements were taken of the cholinergic system and oxidative stress markers. In silico docking was used to find the role of tau protein kinase and phosphatase in the pharmacological action.

Results: In OKA-induced rats, IRJ decreased the escape latency and path length in MWM and increased the exploration time for novel objects and the discrimination index in NORT. ICV-OKA rats had higher free radicals and cytokines that caused inflammation and their level of free radical scavengers was back to normal with IRJ treatment. IRJ increased the level of acetylcholine and inhibited acetylcholinesterase. Moreover, the in silico docking study revealed the strong binding affinity of 10-hydroxy-2-decenoic acid (10-HDA), a bioactive constituent of IR, to the tau protein kinases and phosphatases.

Conclusion: IRJ may serve as a nootropic agent in the treatment of dementia, and owing to its capacity to prevent oxidative stress and neuroinflammation, and increase cholinergic tone; it has the potential to be explored as a novel strategy for the treatment of dementia and AD. More studies may be needed to develop 10-HDA as a novel drug entity for AD.

1. Introduction

Alzheimer's disease (AD) is a progressive neurodegenerative disorder and the most common form of dementia.[1] Worldwide, about 57 million people had dementia in 2019, and it is estimated to increase to 152.8 million cases in 2050.[2] The brains of individuals with AD have an abundance of plaques and tangles made up of beta-amyloid and/or tau proteins.[1] These plaques and tangles develop with age in the brain areas responsible for memory processing and tend to disable or block communication amongst nerve cells.[3] They also initiate processes such as oxidative stress and neuroinflammation that lead to neurodegeneration.[4] Behaviorally, these people exhibit mental dysfunction, impairment of cognitive function, increased apathy, decreased speech, and gait irregularities.[5] Despite the growing population of patients with

Peer review under responsibility of The Center for Food and Biomolecules, National Taiwan University.
* Corresponding author. Department of Pharmaceutical Chemistry, Poona College of Pharmacy, Bharati Vidyapeeth (Deemed to be University), Pune, 411038, Maharashtra, India.
E-mail address: l.satyanarayan@bharatividyapeeth.edu (L. Sathiyanarayanan).

https://doi.org/10.1016/j.jtcme.2023.11.005
Received 6 December 2022; Received in revised form 21 October 2023; Accepted 11 November 2023
Available online 15 November 2023

AD, current therapies are only for symptomatic relief, and there is no treatment available for neuroprotection or reversing the disease progression. Recent advances in therapy targeting the reversal of pathological hallmarks of disease are being achieved with monoclonal antibodies such as aducanumab (approved), donanemab, and lecanemab (in review with the US Food and Drug Administration).[6] However, owing to the side effects associated with synthetic small molecules and monoclonal antibodies, current knowledge recommends the use of micronutrients, supplements, and herbal medicines to relieve AD symptoms and achieve neuroprotection.[7]

Royal jelly (RJ), a bee (*Apis mellifera*) product, is a traditional functional food used to maintain human health.[8] RJ is rich with proteins, carbohydrates, lipids (mainly 10-hydroxy-trans-2-decenoic acid (10-HDA), mineral salts, polyphenols, enzymes, hormones, vitamin-B complexes (such as B1, B2, B6, and biotin), and choline.[9,10] These constituents endow RJ with a variety of pharmacological activities, including anti-inflammation, antioxidant, anti-aging, and neuroprotection/neuromodulation.[11–15] Indeed, RJ improved cognitive impairments in different animal models, such as trimethyltin-treated mice and streptozotocin-induced sporadic AD rat models, and alleviated amyloid-β toxicity in *C. elegans*.[15–17] The bioactive compound of RJ, 10-HDA, has also been reported to induce antibiotic, immunomodulatory, anti-tumor, estrogenic, and neurogenic activity.[18]

The present study evaluated the effect of IRJ on learning and memory in OKA-induced memory deficit rats, a well-validated animal model of AD.[19] Further assessed the involvement of IRJ on oxidative stress, neuroinflammation, and acetylcholine (ACh) regulation and to elucidate the mechanism of action of IRJ, we tested the hypothesis of 10-HDA in regulating the key tau protein kinases viz. glycogen synthase kinase-3β (GSK-3β), cyclin-dependent kinase-5 (CDK-5), and tau protein phosphatase-2A (PP2A) by employing docking studies.[20]

2. Materials and methods

2.1. Chemicals

Indian Royal Jelly (IRJ) samples were obtained from the southern region (IRJ I), the northern region (IRJ II), and the central region (IRJ III) of India. All the samples were authenticated by Central Bee Research and Training Institute, Pune. (See Supplementary Appendix.)

2.2. Animals

Male Wistar rats weighing 250–300g were purchased from Global Science, Pune, Maharashtra, India. Animals were maintained at standard laboratory conditions of 25 °C with 12-h dark and light cycles and free access to food and water *ad libitum*. The experimental protocol for the use of 80 animals was approved by the Institutional Animal Ethics Committee (IAEC), registered with CPCSEA (1703/PO/Re/S/13/CPCSEA), and the protocol approval number was IAEC/PCH01/2021-2022.

2.3. Quantification of 10-HDA and selection of IRJ

The high-performance liquid chromatography (HPLC) technique was used to determine the level of 10-HDA in the IRJ samples. An ACE E5 Amide C-18 column (250 mm × 4.6 mm, 5 μm) was used for method development. The mobile phase composition consisted of phosphate buffer (20 mM; pH 3.0; Methanol:ACN) in the ratio of 40:55:05 v/v/v. (See Supplementary Appendix.)

2.4. Preparation of IRJ

Accurately weighed selected IRJ was transferred into 250 ml volumetric flasks, and 150 ml water was added. The mixture was ultrasonicated with occasional shaking, and the volume was made up to the mark with water (500 mg/ml). The solution was further diluted with water to prepare 100 mg/ml, 200 mg/ml, and 400 mg/ml samples respectively.

2.5. Induction of neurodegeneration by intracerebroventricular injection of OKA

Post-overnight fasting, male Wistar rats were anesthetized with propofol (85 mg/kg) and xylazine (5 mg/kg). The head was positioned in a stereotaxic frame, and the lateral cerebral ventricles (both left and right) were located by using the stereotaxic coordinates: 0.8 mm posterior, 1.3 mm lateral to the midline, and 3.5 mm ventral with respect to the bregma as per the stereotaxic atlas, 3.6 mm ventral.[21] Using Hamilton's syringe, 4 μl of OKA was injected into each ventricle to deliver 100 ng/side. (OKA administration procedure and post-operative care described in Supplementary Materials).

2.6. Experimental design

Fifty animals were administered OKA, and divided into 5 groups (10 rats per group) as neurodegeneration control (OKA + vehicle), standard treatment (OKA + memantine, 10 mg/kg, per oral), and the test (OKA + IRJ, 100, 200, and 400 mg/kg, per oral dose respectively). The drug treatment was initiated on day 7 of the OKA injection and continued for 21 days. Behavioral tests were performed on following days; day 27 actophotometer, days 28–29 novel object recognition test (NORT), and days 30–34 Morris water maze (MWM) test. Each behavioral assay was performed in 6–7 animals per group. Three animals from each group were sacrificed on day 28 for biochemical estimations. Nine animals were sham-operated and used for behavioral (n = 6) and biochemical estimations (n = 3). A schematic workflow of the experimental design is provided in the Supplementary Appendix (Fig. S1).

2.7. Assessment of learning and memory

2.7.1. Novel object recognition test (NORT)

The NORT was performed in three sessions in an open (from the top), uniformly illuminated (100 lux) plexiglass box (40 × 40 × 40 cm) as per the procedure described in the literature.[22,23] Briefly, in session 1 (Day 28), the rats were allowed to explore the apparatus for 10 min without any objects. In session 2 (Day 29), a 5-min familiarization trial (T1) was conducted where each rat was individually placed in the middle of the apparatus and was allowed to explore two identical objects (See details in the Supplementary Appendix). After a 30-min ($T2_{30\text{-min}}$) inter-trial interval (ITI), session 3 was performed. It was a 5-min choice trial (T2) when one of the objects presented in T1 was replaced by a novel object of different texture and shape. A skilled observer who was blind to the various treatments used a stopwatch to record the total cumulative time that rats spent exploring each object during T1 and T2. As this time may be biased by differences in overall levels of exploration, a discrimination index (DI) was then calculated by comparing the time spent exploring the familiar versus the novel during T2 as follows:

DI = [Exploration to novel object (sec) - Exploration to Familiar object (sec)]

/[Exploration to novel object (Sec) + Exploration to Familiar object (sec)]

2.7.2. Morris water maze (MWM) test

The test was conducted in a circular pool (150 cm in diameter, 45 cm in height) filled with water up to a height of 30 cm (water maintained at 25 ± 1 °C and made opaque with the non-toxic paint).[24] The pool was divided into four equal quadrants, and a white platform (10 cm in diameter) was placed in the middle of one of the quadrants referred to as the target quadrant, 1 cm below the water surface, and it remained unaltered throughout the training session. Various cues were placed on the walls of the room and also on the tank to help the animals navigate

and learn.

A day before the commencement of training (Day 29), the rats were individually placed in the pool with no platform for a 60 s habituation trial. Acquisition trials were conducted on days 30–33, 4 trials/day with 10-min inter-trial intervals. The escape latency and distance traveled to reach the platform for each rat were recorded for each trial.[25] The cut-off time was kept at 120 s. On day 34 of the probe trial, the platform was removed, and the time spent by rats in the target quadrant, where the platform was previously placed, was measured for 60 s (For details procedure see Supplementary Materials.)

2.8. Preparation of brain samples for biochemical profiling

On day 28 of the study, the animals were humanely sacrificed, and the whole brain was dissected. After cleaning with isotonic saline, the brain was crushed and then homogenized with cold phosphate-buffered saline (30 mM, pH 7.4). The homogenate was spun down to get rid of dead cells, and the supernatant was used to estimate biomarkers of oxidative stress, neuroinflammation, and cholinergic neurotransmission [ACh, ACh esterase (AChE)].[26–30] The protein content of the brain was determined following the method of Lowry et al. (1951).[31] Estimation was performed by the colorimetric spectroscopic method or enzyme-linked immunosorbent assay (ELISA) technique. (For detailed procedure see Supplementary Material).

2.9. Histopathological examination of brain tissue sections

Rats (n = 5) were sacrificed from each group on day 35 under thiopentone anesthesia, followed by *trans*-cardiac perfusion with phosphate-buffered saline and then formalin as a fixative. The skull was opened, and the whole brain was excised and stored overnight in 10% formalin, then embedded in paraffin for 4 h. Coronal sections of the brain (5 μm) were cut using paraffin blocks through the hippocampus region using a microtome. Sections were mounted on silane-coated slides. The sections were washed in xylene for deparaffinization, rehydrated in graded ethanol, and finally stained with hematoxylin-eosin (HE).[32] Hippocampal neuron morphology for neuronal loss was observed in 25 (5 sections from each rat brain) random regions in the CA1 subdivision of the hippocampus under a high microscopic field (40X) per group. In these slides, necrotic and/or degenerated neurons in each selected region were descriptively analyzed but not quantified.

2.10. Molecular docking study

The protein data bank was used to get the X-ray crystallographic structures of protein kinases like glycogen synthase kinase-3 (4ACC), cyclin-dependent kinase 5 (3O0G), and tau protein phosphatase 2A (2IAE).[33] The ligand docking was carried out using the Auto dock Vina software (MGL Tool 1.5.7). The visualization of the docking site was enhanced using Discovery Studio. The protein grid was generated with all default parameters around the selected proteins (Table S1). Aloisine A, memantine, and 10-HDA ligands were prepared using ChemBio 3D Ultra 14.0 software 14.0, and the energy was minimized by macromodel multiple minimizations (Table S2). Further, the chemical properties of ligands were obtained using ChemBio 3D Ultra 14.0 (Table S3).

2.11. Statistical analysis

All results were expressed as mean ± SEM. Results were analyzed either by employing the Student's t-test, one-way analysis of variance (ANOVA), or a two-way ANOVA followed by a post hoc test, depending on the type of data, using GraphPad Prism software (version 8.3.0). $P < 0.05$ was considered statistically significant.

3. Results

3.1. Estimation of 10-HDA by HPLC

HPLC analysis of 10-HDA showed the presence of a single peak at 6.03 min and the internal standard alpha-naphthol appeared at 14.02 min (Fig. 1A). Injection of IRJ showed a peak at 6.03 min confirming the presence of 10-HDA. (Fig. 1B). Quantification of total 10-HDA content in three samples of IRJ showed different levels of 10-HDA: IRJ I - 2.021 ± 0.018%; IRJ II - 2.310 ± 0.011% and IRJ III - 1.295 ± 0.021% (Fig. 1B Insets). This indicated that IRJ II contains higher quantity of 10-HDA, and therefore IRJ II was selected for further pharmacological evaluations.

3.2. Effect of IRJ on recognition memory

During the familiarization trial (T1), animals spent approximately equal time exploring both objects, and no differences were observed in the total exploration time across the groups. In the choice trial (Fig. 2A), sham-controlled rats explored the novel object for a significantly longer duration than the familiar object, indicating intact memory ($P < 0.001$). In the OKA group, rats spent approximately equal time exploring familiar and novel objects. IRJ (200 and 400 mg/kg) treatment of the OKA-treated rats explored the novel object for a significantly longer duration than the familiar object ($P < 0.01$) and the response was comparable to that of the control group. This suggests that IRJ at higher doses reverses short-term recognition memory deficits in OKA-treated rats. The effect of IRJ at higher doses (200 and 400 mg/kg) was comparable to that of memantine, which showed a significantly longer duration of exploration of the novel object than the familiar one ($P < 0.001$).

DI was calculated based on the exploratory behavior of rats during a choice trial (Fig. 2B). One-way ANOVA revealed a significant effect of IRJ and memantine on DI [$F(5,30) = 18.25$, $P < 0.001$]. Post hoc Dunnett's multiple comparison tests suggested that IRJ significantly (200 mg/kg, $P < 0.01$ and 400 mg/rat, $P < 0.001$) increased the DI as compared with that of the OKA group, similar to memantine ($P < 0.001$). However, a lower dose of IRJ (100 mg/kg) did not alter the DI as compared to that of the control group.

3.3. Effect of OKA on MWM performance

In the acquisition trial, treatment with memantine and IRJ significantly decreased the escape latency in OKA-treated rats (Fig. 2C). A two-way ANOVA showed a significant effect of factors like 'treatment' [$F(1,48) = 3.864$, $P < 0.05$] 'days' [$F(3,48) = 13.89$, $P < 0.001$ on spatial memory deficits in rats. However, the interaction 'OKA treatment' x 'acquisition days' was not significant [$F(3,48) = 10784$, $P < 0.1628$]. Results revealed that normal animals (sham-operated) showed a gradual decrease in the escape latency from days 1–4 of the acquisition trial, and this reduction was significant on day 3 ($P < 0.01$) and day 4 ($P < 0.001$). On the other hand, a mild decrease in escape latency was observed in the OKA treatment group. In addition, a within-group comparison showed that escape latency in the sham-operated group was significantly decreased on days 3 ($P < 0.05$) and days 4 ($P < 0.01$) as compared to that in the OKA group. This suggested that OKA induced deficits in the spatial learning of rats.

Treatment with memantine (10 mg/kg, po) in OKA-treated rats produced a significant effect on increasing escape latency [two-way ANOVA, 'treatment' $F(1,48) = 17.90$, $P < 0.0001$; 'days' $F(1,48) = 21.21$, $P < 0.0001$ and the interaction 'treatment' x 'days' $F(3,48) = 4.369$, $P < 0.01$] (Fig. 2D). It showed a gradual decrease in the escape latency from days 1–4 of the acquisition trial (days 3 and 4, $P < 0.001$ vs. OKA rats). In addition, a within-group comparison showed that escape latency in the OKA + memantine group was significantly decreased on days 3 ($P < 0.05$) and 4 ($P < 0.01$) as compared to that in the OKA group

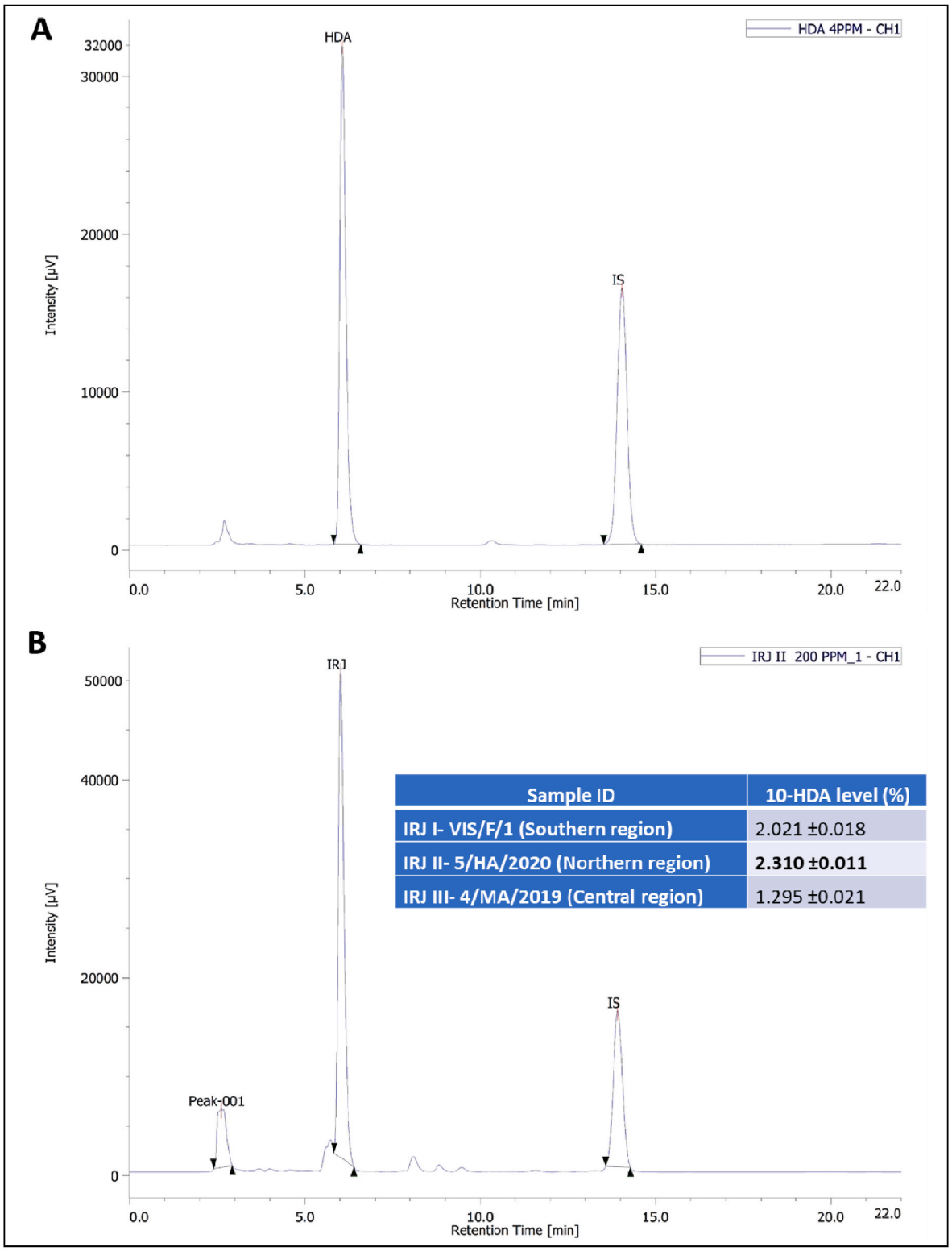

Fig. 1. Representative high-performance liquid chromatography profile of standard 10-HDA (A) and Indian royal jelly (IRJ, B). Alpha-naphthol was used as internal standard (IS). Peak was obtained at same time after 10-HDA or IRJ sampling at 6.03 min and for IS at 14.02 min. Quantification assay showed the highest concentration of 10-HDA in IRJ II (Inset).

alone.

Similarly, treatment with IRJ (100, 200, and 400 mg/kg, po) resulted in a significant decrease in the escape latency in OKA-treated rats [two-way ANOVA, 'treatment' $F(3,96) = 6.186$, $P < 0.0001$; 'days' $F(3,96) = 40.29$, $P < 0.0001$ and the interaction 'treatment' x 'days' $F(9,96) = 1.064$, $P = 0.3965$] (Fig. 2C). A significant decrease in the escape latency was observed as early as day 2 in the IRJ 400 mg/kg treatment group ($P < 0.05$). The effect was highly significant on days 3 and 4 ($P < 0.001$) in IRJ 200 and 400 mg/kg treatment groups as compared to the respective time periods in the OKA group ($P < 0.01$ and $P < 0.001$). A lower dose of

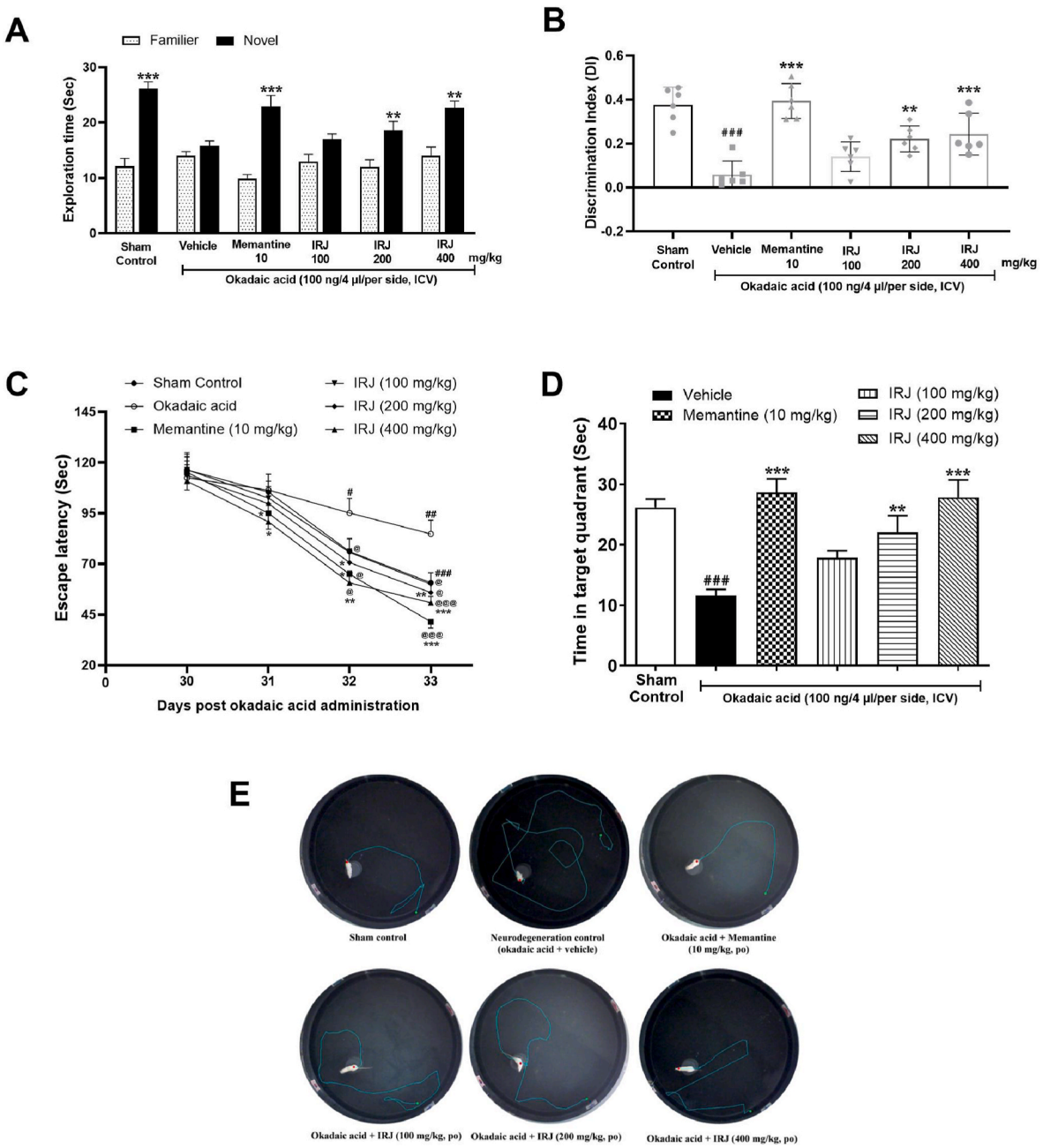

Fig. 2. Effects of memantine and IRJ on recognition (A,B) and spatial (C–E) learning and memory in okadaic acid (OKA) induced rat model of neurodegeneration. **A.** Exploration time of rats to familiar and novel objects during choice trial and Mean (Sec) ± SEM was statistically compared for significance using Student's t-test (**p < 0.01, ***p < 0.001). **B.** Discrimination index by employing One-way ANOVA followed by Dunnett's multiple comparison test ($^{###}$p < 0.001 vs Sham-operated group; **P < 0.01 and ***P < 0.001 vs OKA). **C.** Escape latency (Sec) effect was statistically compared by employing Two-way ANOVA followed by Tukey's multiple comparison post hoc test ($^{@}$p < 0.05, $^{@@@}$p < 0.001 vs day 1 within the same group; $^{\#}$p < 0.05, $^{\#\#}$p < 0.01 vs Sham-operated group; *p < 0.05, **p < 0.01, ***p < 0.001 vs respective days in OKA group). **D.** Represents the mean time spend in each target quadrant ($^{###}$p < 0.001 vs Sham-operated group; **p < 0.01 and ***p < 0.001 vs OKA. **E.** Path length of rats on day 4 of acquisition trial. Analysis of path length was descriptive.

IRJ (100 mg/kg) did not produce a significant effect on learning behavior (P > 0.05).

The effect of IRJ in the acquisition trial was also reflected in the probe test (Fig. 2D). IRJ dose-dependently increased the time spent in the target quadrant when compared with that of the control group [F (5,35) = 10.19, P < 0.001]. A significant effect was noticed with IRJ treatment at 200 mg/kg (P < 0.01) and 400 mg/kg (P < 0.001) doses. The lower dose (100 mg/kg), however, did not produce a significant effect on memory performance (P > 0.05). The effect of IRJ at a higher dose (400 mg/kg) was comparable to that of memantine which showed increased time spent by rats in the target quadrant as compared to the OKA group (P < 0.001).

A reduction in the distance traveled to reach the platform was observed during the consecutive days of the acquisition phase. The path length is indicative of the distance traveled on day 4 (trial 4) as shown in Fig. 2E. ICV-OKA-treated rats covered longer distances than the sham control rats. Rats in the IRJ or memantine group achieved better results than OKA-treated animals as they covered a significantly shorter distance to find the platform.

3.4. Effect of IRJ on AChE inhibition and the levels of ACh

IRJ and memantine were both effective in inhibiting AChE activity (Fig. 3A). Memantine showed 37.33% inhibition of AChE activity. IRJ also showed a dose-dependent effect on AChE inhibition, where 17.67%, 29.09%, and 38.65% inhibition were observed with IRJ 100, 200, and 400 mg/kg, respectively.

Fig. 3B represents the effects of IRJ or memantine treatment on AChE activity [$F(5,30) = 13.03$, $P < 0.001$]. While OKA treatment significantly reduced the ACh level as compared to sham-operated rats ($P < 0.001$), IRJ treatment restored the level of ACh in the OKA rats (200 mg/kg $P < 0.05$ and 400 mg/kg $P < 0.01$); effect similar to memantine

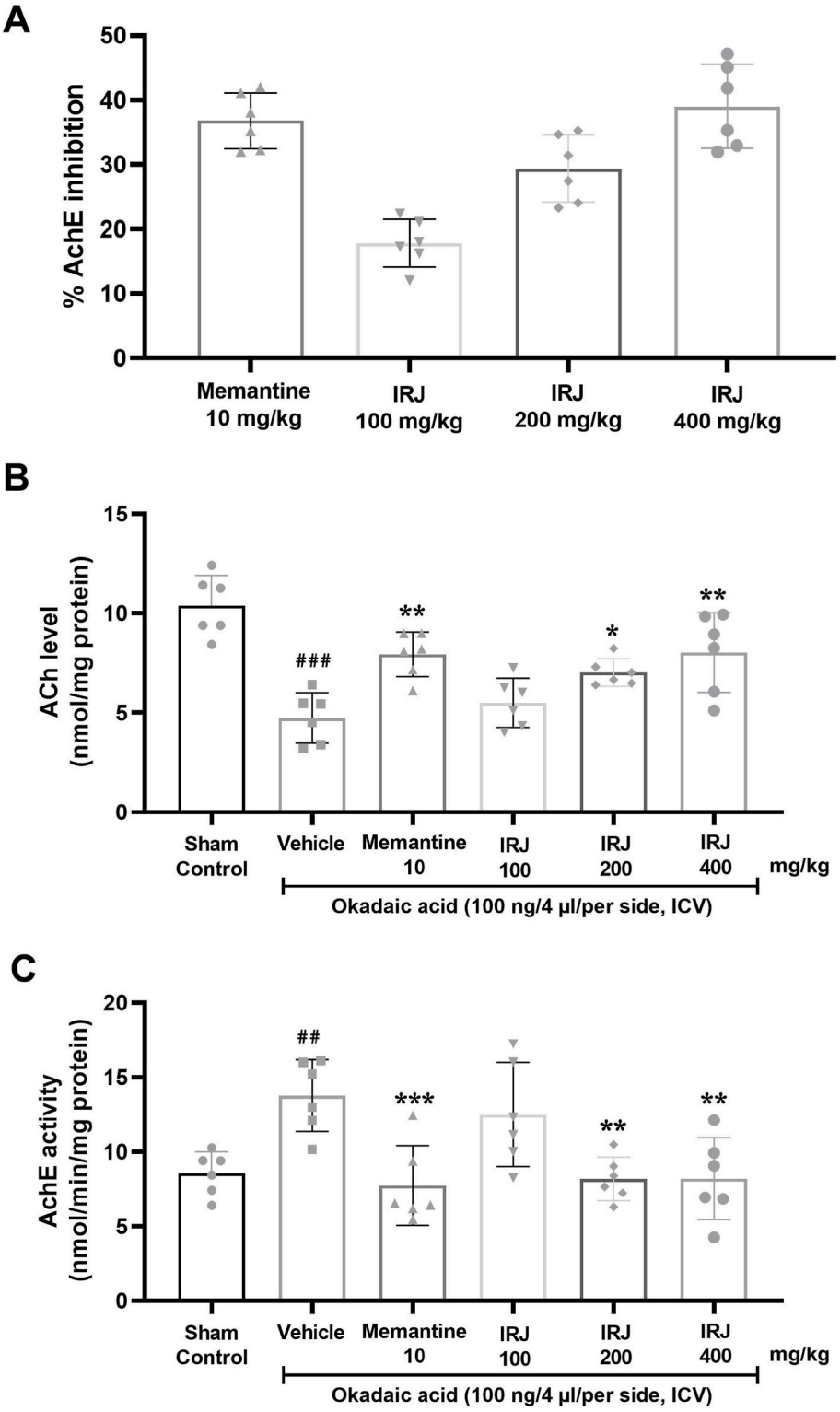

Fig. 3. Effect of oral treatment with memantine (10 mg/kg) and IRJ (100, 200 and 400 mg/kg) on acetylcholinesterase (AChE) inhibition (A), acetylcholine level (B) and AChE activity (C) in the brain. Values were expressed as mean ± SEM. $^{\#\#}p < 0.01$ and $^{\#\#\#}p < 0.001$ vs Sham-operated group; $^{*}p < 0.05$, $^{**}p < 0.01$ and $^{***}p < 0.001$ vs OKA group. (One-way analysis of variance followed by Dunnett's multiple comparison post hoc test).

treatment ($P < 0.01$). Fig. 3C showed a significant effect of IRJ and memantine treatment on AChE activity [$F(5,30) = 6.63$, $P < 0.001$]. In the OKA treatment group, AChE activity was increased compared to the sham control group ($P < 0.01$). IRJ (IRJ 200 mg/kg and 400 mg/kg $P < 0.01$ or memantine ($P < 0.001$) treatment inhibited the AChE activity in these rats.

3.5. Effect of IRJ on the oxidative stress biomarkers

The different biomarkers, such as NO, MDA, GSH, SOD, and catalase, play a key role in the oxidation cascade. Drug treatment showed NO levels significantly increased in the OKA group [$F(5,30) = 6.889$, $P < 0.001$]. Memantine ($P > 0.05$) as well as IRJ (IRJ - 200 mg/kg $P < 0.05$; IRJ - 400 mg/kg $P < 0.01$) significantly decreased the NO level in OKA pretreated rats (memantine – $P > 0.05$; (Fig. 4A).

The effect of OKA and drug treatment was also significant on the modulation of the level of MDA in the brain [$F(5,30) = 7.388$, $P < 0.001$]. OKA significantly increased the level of MDA in the brain as compared to the sham group ($P < 0.001$). On the other hand, memantine ($P < 0.01$) as well as IRJ (200 mg/kg $P < 0.05$; 400 mg/kg $P < 0.01$) significantly reduced the level of MDA in the OKA-treated rats (Fig. 4B).

Memantine or IRJ in the OKA-treated rats produced a significant effect on the levels of GSH [$F(5,30) = 5.933$, $P < 0.001$], SOD [$F(5,30) = 8.825$, $P < 0.001$] and catalase [$F(5,30) = 4.447$, $P < 0.01$] in the brain as compared to the sham-operated rats (Fig. 4C–E). Memantine restored the levels of these biomarkers in the OKA-treated rats (all $P < 0.05$). Similarly, IRJ treatment also increased the levels of GSH (200 mg/kg $P < 0.05$; 400 mg/kg $P < 0.01$), SOD (200 mg/kg $P < 0.05$; 400 mg/kg $P < 0.01$), and catalase (both dose $P < 0.05$) significantly as compared to the OKA group.

3.6. Effect of IRJ on the expression of proinflammatory cytokines (IL-1β, IL-6, and TNF-α)

One-way ANOVA revealed a significant effect of OKA administration and treatment of IRJ or memantine on IL-1β [$F(5,30) = 13.42$, $P < 0.001$; Fig. 5A], IL-6 [$F(5,30) = 10.77$, $P < 0.001$; Fig. 5B] and TNF-α [$F(5,30) = 43.85$, $P < 0.001$; Fig. 5C]. Memantine was effective in significantly restoring the level of these cytokines as to that of the sham-operated rats (IL-1β $P < 0.05$, IL-6 $P < 0.01$ and TNF-α $P < 0.001$). A

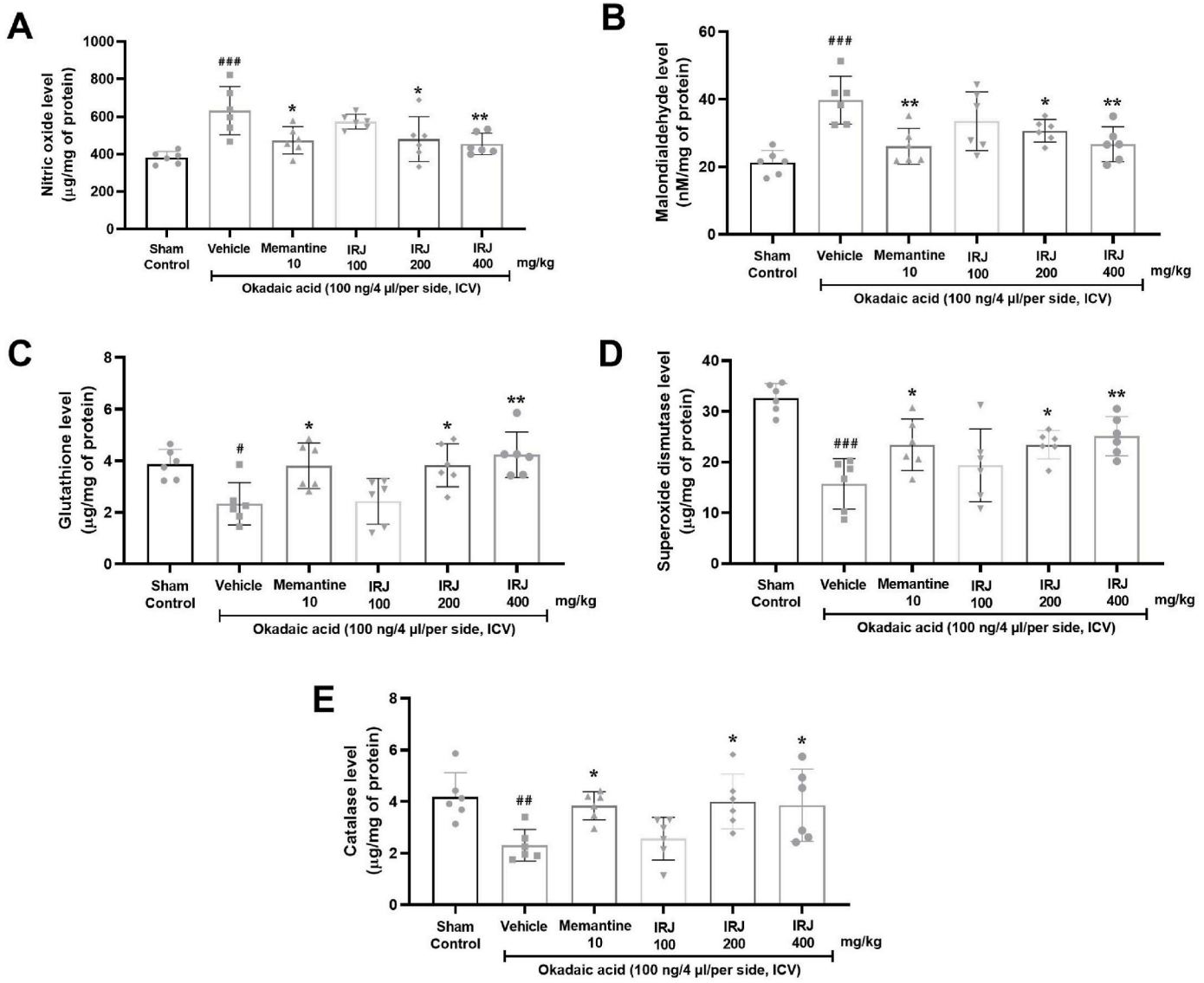

Fig. 4. Effect of oral memantine (10 mg/kg) and IRJ (100, 200 and 400 mg/kg) treatment on nitric oxide (A), malondialdehyde (B), reduced glutathione (C), superoxide dismutase (D) and catalase (E) activity in brain. Values were expressed as mean ± SEM. $^{\#}p < 0.05$, $^{\#\#}p < 0.01$ and $^{\#\#\#}p < 0.001$ vs Sham-operated group; $^{*}p < 0.05$, $^{**}p < 0.01$ and $^{***}p < 0.001$ vs OKA group. (One-way analysis of variance followed by Dunnett's multiple comparison post hoc test).

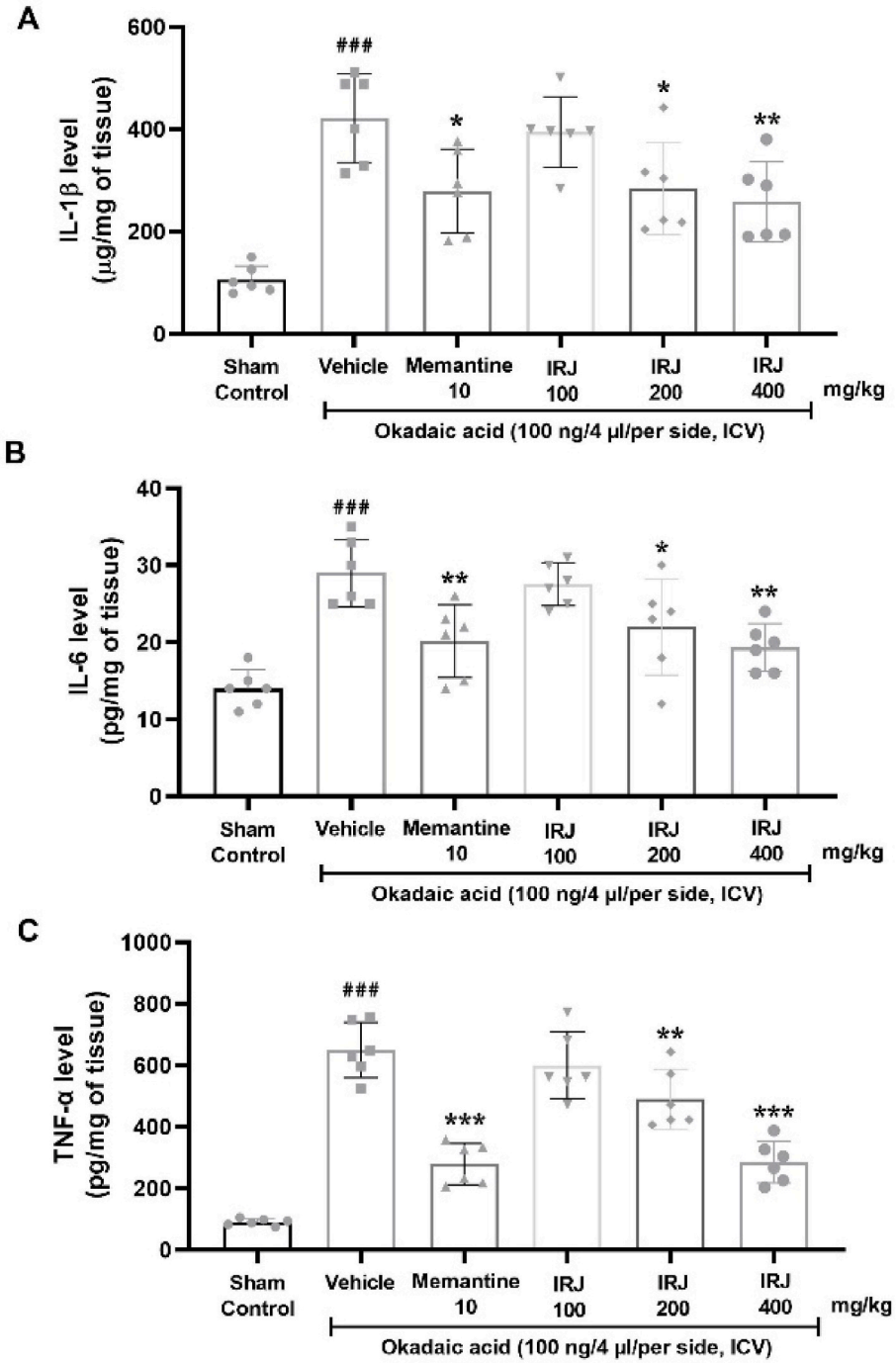

Fig. 5. Effect of oral treatment with memantine (10 mg/kg) and IRJ (100, 200 and 400 mg/kg) on interleukin (IL)-1β (A), IL-6 (B) and tumor necrotic factor-α (TNF-α, C) level in the brain. Values were expressed as mean ± SEM. $^{###}p < 0.001$ vs Sham-operated group; *$p < 0.05$, **$p < 0.01$ and ***$p < 0.001$ vs OKA group.

similar effect was noted with higher doses of IRJ. IRJ significantly decreased the IL-1β (200 mg/kg $P < 0.05$ and 400 mg/kg $P < 0.01$), IL-6 (200 mg/kg $P < 0.05$ and 400 mg/kg $P < 0.01$), and TNF-α (200 mg/kg $P < 0.01$ and 400 mg/kg $P < 0.001$).

3.7. Effects of IRJ on pathological changes in the rat hippocampus

HE staining was employed to identify the morphologically intact neurons in the CA1 region of the hippocampus. On day 34, in the hippocampus of the ICV-OKA rats (Fig. 6A), we observed pyramidal cells with irregular or shrunken shapes and deeper staining. Qualitatively the condition was worse than the sham control rats (Fig. 6B). Treatment with memantine (Fig. 6C) and IRJ (Fig. 6D) reduced the number of dead cells seen as shrunken or irregular shape and deeper staining in the ICV-OKA rats.

3.8. Molecular docking of IRJ as a tau protein kinase inhibitor

The complex of Aloisine A, memantine, and 10-HDA with the inhibitory binding sites in the enzymes protein kinase and protein phosphatase is shown in (Fig. 7). All molecules interacted at the active sites of enzymes 4ACC, 3O0G, and 2IAE through bonds like hydrogen, van der Waals, alkyl, π-alkyl, π-donor hydrogen, carbon-hydrogen bond, π-σ, π-π stacked and π-π T shaped and showed comparatively good

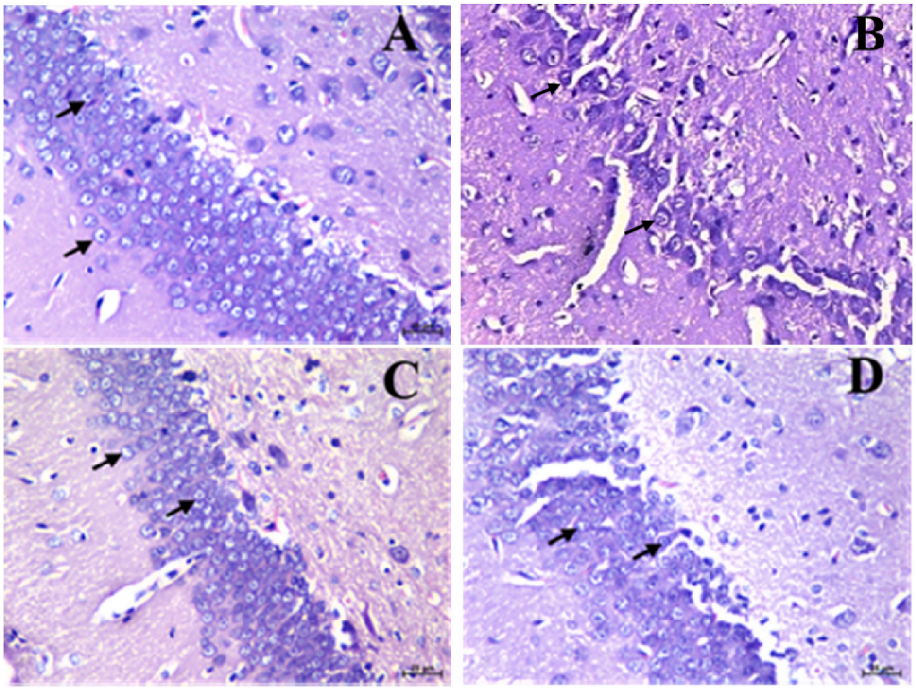

Fig. 6. Brain sections through hippocampus regions processed for hematoxylin and eosin staining. A. Normal control group, B. OKA control group, C. OKA-memantine (10 mg/kg) and D. OKA-IRJ (400 mg/kg). Small arrows are pointed at normal and degenerated neurons. Images were captured at 40X magnification.

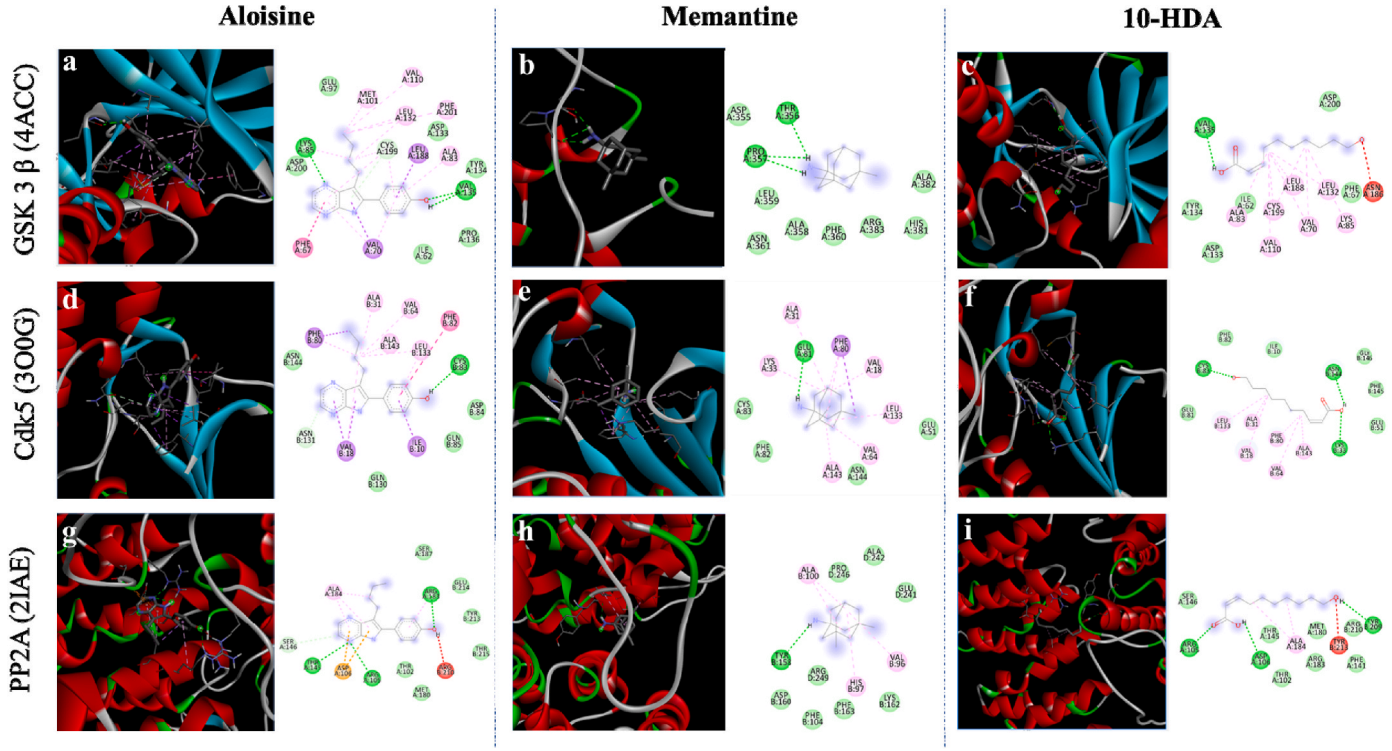

Fig. 7. The figure represents docking zone of ligands aloisine A (a, d and g), memantine (b, e and h) and 10-HDA (c, f, and i) bonded with enzyme glycogen synthase kinase-3 (GSK-3β, 4ACC), cycline-dependent kinase-5 (Cdk5, 3O0G) and tau protein phosphatase-2A (PP2A, 2IAE) in 2D and 3D.

binding energy (Table 1). Docking results indicated the binding similarities of Aloisine A and 10-HDA. This suggests the affinity of 10-HDA towards the inhibitory binding sites of the enzyme protein kinase and protein phosphatase.

4. Discussion

There are different types of royal jelly, which differ in their constituents and quality. Quality-wise, IRJ is comparable to the best in the world. The present study showed for the first time that IRJ significantly improves learning and memory deficits in ICV-OKA-induced AD rats.

Table 1
Binding profile of aloisine, memantine and 10-HDA at binding site of tau protein kinase and tau protein phosphatase.

	Binding of compound to GSK-3β (4ACC)			Binding of compound to CDK-5 (3O0G)			Binding of compound to PP2A (2IAE)		
	Binding energy	Chain A	Chain B	Binding energy	Chain A	Chain B	Binding energy	Chain A	Chain B
Aloisine A	−7.9	VAL-135, LYS-85, PHE-67, VAL-70, LEU-188, ALA-83, CYS-199, MEP-101, VAL-110, LEU-132, PHE-201	Nil	−8.2	Nil	CYS-83, PHE-82, ILE-10, VAL-18, PHE-80, ASN-131, ALA-31, ALA-143, LEU-133, VAL-64	−6.8	ASP-106, SER-146, THR-145, ARG-105, ARG-183, ALA-184	ARG-210
Memantine	−5.4	PRO-357, THR-356	Nil	−7.2	GLU-81, ALA-31, LYS-33, ALA-143, VAL-64, LEU-133, VAL-18, PHE-80	Nil	−6.9	Nil	THR-158, HIS-97, VAL-96, ALA-100, TYR-216, TYR-209
10-HDA	−5.2	VAL-135, ALA-83, VAL-110, CYS-199, LEU-188, VAL-70, LEU-132, LYS-85, ASN-186	Nil	−5.8	Nil	CYS-83, ASN-144, LYS-33, ALA-143, VAL-64, PHE-80, VAL-18, ALA-31, LEU-133	−5.2	ASP-106, ARG-105, ALA-184,	Nil

10-HDA, 10-hydroxy-trans-2-decenoic acid; CDK-5, cyclin-dependent kinase-5; GSK-3β, glycogen synthase kinase-3β; PP2A, tau protein phosphatase-2A.

HPLC is the economical and preferred analytical technique for the determination of various essential components of extracts. Quantification using HPLC showed the presence of varying levels of 10-HDA in IRJ samples obtained from different geographical locations in India. Quantification showed that IRJ from the northern region contained the highest percentage of 10-HDA and therefore we used the same sample for further studies.

Clinical observation showing memory impairment in human subjects who eat seafood contaminated with dinoflagellate, the major source of OKA, prompted the use of OKA in the development of animal models for cognitive deficits.[34,35] Indeed, OKA administered directly in the brain potently induces learning and memory impairment in addition to the formation of β-amyloid-containing plaque-like structures and hippocampal neurodegeneration.[36] Similar deficits in spatial as well as recognition memory were observed in rats who were administered OKA in the lateral cerebral ventricles. These rats spent approximately equal time exploring the familiar and novel objects and showed higher escape latency while locating the platform, which reflected their inability to recognize the events or spatial cues.

RJ is reported to be effective in improving spatial learning and memory. However, different types of RJ have shown different pharmacological profiles.[15,37,38] While the escape latency in ICV-OKA rats during the acquisition trial in the MWM test from day 1 to day 4 did not decrease significantly, IRJ significantly reduced the escape latency in ICV-OKA-administered rats. The loss of spatial working memory is one of the early signs of AD. IRJ treatment after OKA-induced damage may exert symptomatic relief by improving spatial learning and memory, similar to memantine. We used memantine as a positive control. There are also studies demonstrating the positive effect of chronic administration of memantine on attenuating OKA-induced spatial short-term memory impairment and the neuropathological changes in the hippocampus. It is also suggested that OKA can be used as an experimental model and it is validated using memantine as a memory enhancer as well as neuroprotective.[39] Other variants of RJ, such as Greek RJ failed to improve spatial memory despite affecting neurotransmission, suggesting the pharmacological superiority of IRJ.[38] In the additional behavioral assay used to assess recognition memory, ICV-OKA rats could not recognize the novel object presented during the choice trial. This indicates the loss of short-term recognition memory by OKA.[40] On the other hand IRJ treatment from day 7 of OKA injection improved the ability to recognize novel objects, indicating intact recognition memory. Locomotor behavior in disease and treatment groups was not altered, suggesting that IRJ treatment did not produce a CNS stimulant or depressant effect (Fig. S4). This also ruled out the possibility that locomotor behavior produces a confounding effect on MWM or NORT. To our knowledge, this is the first study to demonstrate the efficacy of any kind of RJ on recognition memory. Since over the course of AD different types of memories get impaired gradually, the use of IRJ may exert symptomatic relief irrespective of the type of memories affected in people with AD.

According to the cholinergic hypothesis, degeneration of cholinergic neurons leads to decreased ACh along with the increased activity of AChE in the brain resulting into cognitive impairment in AD.[41,42] Microinfusion of OKA into the rat brain induces neurodegeneration and neurotoxicity, leading to central cholinergic dysfunction, which is a plausible mechanism of memory impairment.[43] We also observed a reduced level of rats' ACh and increased AChE activity in ICV-OKA-treated rats. IRJ increased the ACh level and reduced the AChE activity, showing activation of cholinergic tone in OKA rats. Memantine produced a similar effect on cholinergic activity as reported previously.[43] Based on these results, it seems that IRJ is able to increase or restore cholinergic activity in the AD model in rats. This suggests that IRJ could be used to treat AD-like diseases or dementias that are caused by cholinergic dysfunction.

Behavioral consequences of AD start with the neuropathological changes in the brain. ICV-OKA is also linked to significant increase in lipid peroxide and NO levels and decrease in the activities of GSH, SOD, and catalase in rats, which is similar to what other studies have found.[19] Oxygenated radicals affect energy conservation mechanisms, and post-translation modification of proteins to ultimately cause neuronal cell death in AD.[44] Antioxidant substances play an important role in scavenging those free radicals and, therefore may alleviate apoptosis and prevent neurodegeneration.[45] IRJ decreased the level of NO and MDA and increased the free radical scavengers, viz., GSH, SOD, and catalase. IRJ, by activating these enzymes, contributed to neuroprotection in AD-like neurodegenerative pathologies.

Neuroinflammation is another pathological hallmark of AD brains and is associated with significant imbalances in the anti-inflammatory versus pro-inflammatory cytokines (IL-1β, IL-6, and TNF-α).[46] OKA administration also increased levels of IL-1β, IL-6, and TNF-α.[41] IRJ treatment following OKA inhibited the level of IL-1β, IL-6, and TNF-α indicating anti-inflammatory function. Previously, the inhibitory effect of RJ on proinflammatory cytokines was reported in *in-vitro* assays such as lipopolysaccharide-induced inflammation in BV-2 microglial cells.[11] The anti-inflammatory effects of IRJ offer a new dimension in the mechanism of action of IRJ for AD.[47] In parallel to cognitive improvement, reducing oxidative stress and neuroinflammation markers, IRJ treatment also prevented OKA-induced morphological damage in the hippocampus. IRJ reduced the loss of neuronal cells in this brain area. This suggested the role of IRJ in neural protection against OKA-induced AD rats.

The principal constituent of the IRJ and its therapeutic target that

accounts for this neuroprotective action is unknown. The animal experiments and biochemical evaluation along with *in vitro* assays in this study demonstrated that IRJ is an effective nootropic agent following brain damage with OKA, as it prevents oxidative stress and neuroinflammation, and increase cholinergic tone. HPLC estimation demonstrated that 10-HDA is the major constituent in IRJ. Based on this we hypothesized that the biological effects of IRJ might be owned mainly by 10-HDA, one of the main lipid constituents of the IRJ. In the molecular docking experiments, we selected 10-HDA as a ligand against biological targets (tau kinase and phosphatase). The binding affinity of 10-HDA towards key protein kinases such as GSK-3β, CDK-5, and PP2A was determined by molecular docking studies. GSK-3β, CDK-5, and PP2A have been extensively studied for their roles in the clinical manifestations of AD, including the production of Aβ plaques, hyperphosphorylation of tau protein, and neurodegeneration.[48,49] OKA is attributed to its PP2A inhibition, induces tau hyperphosphorylation and neurodegeneration *in-vitro* and *in-vivo*. GSK3β phosphorylation is also observed in the AD brain in OKA model.[50] Similar to aloisine A and memantine, 10-HDA binds to these targets at its inhibitory sites. This suggest that the effect of IRJ may be attributed to the capacity of 10-HDA in the inhibition of tau kinases and phosphatases such as GSK-3β, CDK-5, and PP2A which are involved in the tau processing in the brain.

5. Conclusion

We demonstrated that IRJ treatment improved learning and memory in OKA-induced AD rat models. In this model, IRJ was effective in regulating oxidative stress, and neuroinflammation, preventing neuronal loss and cholinergic dysfunction. This effect may be attributed to the major constituent of the IRJ, 10-HDA, which may bind to the tau protein kinases to prevent hyperphosphorylation. Overall the finding suggests the neuroprotective effect of IRJ in the prevention of AD-like conditions.

Conflicts of interest

None.

Funding

This work was financially supported by the All-India Council for Technical Education, Government of India through the Quality Improvement Programme (File no: DIPSAR/AICTE/QIP/Nodal/C.L./2018/1205 Year 2018).

Declaration of competing interest

Rahul N. Dubey, Sathiyanarayanan L, Sandeep Sankaran and Arulmozhi S declare that they have no conflict interests to declare that are relevant to the work reported in this manuscript.

Acknowledgement

We express our gratitude towards The Director, Central Bee Research and Training Institute, Pune, for supporting this work. We also like to thank Ashish Bharne, Ph.D., for his support in statistical analysis, compilation of results and editing of the manuscript.

Appendix A. Supplementary data

Supplementary data to this article can be found online at https://doi.org/10.1016/j.jtcme.2023.11.005.

References

1. Jeong S. Molecular and cellular basis of neurodegeneration in alzheimer's disease. *Mol Cell*. 2017;40(9):613–620.
2. GBD 2019 Dementia Forecasting Collaborators. Estimation of the global prevalence of dementia in 2019 and forecasted prevalence in 2050: an analysis for the Global Burden of Disease Study 2019. *Lancet Public Health*. 2022;7(2):e105–e125.
3. Wang JZ, Wang ZH, Tian Q. Tau hyperphosphorylation induces apoptotic escape and triggers neurodegeneration in Alzheimer's disease. *Neurosci Bull*. 2014;30(2):359–366.
4. Rehman IU, Ahmad R, Khan I, et al. Nicotinamide ameliorates amyloid beta-induced oxidative stress-mediated neuroinflammation and neurodegeneration in adult mouse brain. *Biomedicines*. 2021;9(4):408.
5. Cerejeira J, Lagarto L, Mukaetova-Ladinska EB. Behavioral and psychological symptoms of dementia. *Front Neurol*. 2012;3:73.
6. Avgerinos KI, Ferrucci L, Kapogiannis D. Effects of monoclonal antibodies against amyloid-β on clinical and biomarker outcomes and adverse event risks: a systematic review and meta-analysis of phase III RCTs in Alzheimer's disease. *Ageing Res Rev*. 2021;68, 101339.
7. Soheili M, Karimian M, Hamidi G, Salami M. Alzheimer's disease treatment: the share of herbal medicines. *Iran J Basic Med Sci*. 2021;24(2):123–135.
8. Sabatini AG, Marcazzan GL, Caboni MF, Bogdanov S, Almeida-Muradian LBD. Quality and standardisation of royal jelly. *J Apiproduct Apimedical Sci*. 2009;1:16–21.
9. Karaali A, Meydanoglu F, Eke D. Studies on composition, freeze-drying and storage of Turkish royal jelly. *J Apicult Res*. 1988;27:182–185.
10. Guo J, Wang Z, Chen Y, et al. Active components and biological functions of royal jelly. *J Funct Foods*. 2021;82, 104514.
11. You MM, Chen YF, Pan YM, et al. Royal Jelly Attenuates LPS-Induced inflammation in BV-2 microglial cells through modulating NF-κB and p38/JNK signaling pathways. *Mediat Inflamm*. 2018;2018, 7834381.
12. Guo H, Kouzuma Y, Yonekura M. Structures and properties of antioxidative peptides derived from royal jelly protein. *Food Chem*. 2009;113:238–245.
13. Honda Y, Araki Y, Hata T, et al. 10-Hydroxy-2-decenoic acid, the major lipid component of royal jelly, extends the lifespan of Caenorhabditis elegans through dietary restriction and target of rapamycin signaling. *J Aging Res*. 2015;2015, 425261.
14. Hashimoto M, Kanda M, Ikeno K, et al. Oral administration of royal jelly facilitates mRNA expression of glial cell line-derived neurotrophic factor and neurofilament H in the hippocampus of the adult mouse brain. *BiosciBiotechnolBiochem*. 2005;69:800–805.
15. Zamani Z, Reisi P, Alaei H, Pilehvarian AA. Effect of royal jelly on spatial learning and memory in rat model of streptozotocin-induced sporadic Alzheimer's disease. *Adv Biomed Res*. 2012;1:26.
16. Hattori N, Ohta S, Sakamoto T, Mishima S, Furukawa S. Royal jelly facilitates restoration of the cognitive ability in trimethyltin-intoxicated mice. *Evid Based Complement Alternat Med*. 2010;2011, 165968.
17. Wang X, Cao M, Dong Y. Royal jelly promotes DAF-16-mediated proteostasis to tolerate β-amyloid toxicity in C. elegans model of Alzheimer's disease. *Oncotarget*. 2016;7:54183–54193.
18. Sugiyama T, Takahashi K, Mori H. Royal jelly acid, 10-hydroxy-trans-2-decenoic acid, as a modulator of the innate immune responses. *Endocr, Metab Immune Disord: Drug Targets*. 2012;12(4):368–376.
19. Kamat PK, Rai S, Nath C. Okadaic acid induced neurotoxicity: an emerging tool to study Alzheimer's disease pathology. *Neurotoxicology*. 2013;37:163–172.
20. Benitez-King G, Tunez I, Bellon A, Ortiz GG, Anton-Tay F. Melatonin prevents cytoskeletal alterations and oxidative stress induced by okadaic acid in N1E-115 cells. *Exp Neurol*. 2003;182(1):151–159.
21. Paxinos G, Watson C. *The Rat Brain in Stereotaxic Coordinates*. third ed. USA: Academic Press; 1998.
22. Ennaceur A. One-trial object recognition in rats and mice: methodological and theoretical issues. *Behav Brain Res*. 2010;215:244–254.
23. Bharne AP, Borkar CD, Bodakuntla S, Lahiri M, Subhedar NK, Kokare DM. Pro-cognitive action of CART is mediated via ERK in the hippocampus. *Hippocampus*. 2016;26(10):1313–1327.
24. Vorhees CV, Williams MT. Morris water maze: procedures for assessing spatial and related forms of learning and memory. *Nat Protoc*. 2006;1(2):848–858.
25. Pereira IT, Burwell RD. Using the spatial learning index to evaluate performance on the water maze. *Behav Neurosci*. 2015;129(4):533–539.
26. Li J, Wang G, Liu J, et al. Puerarin attenuates amyloid-beta-induced cognitive impairment through suppression of apoptosis in rat hippocampus in vivo. *Eur J Pharmacol*. 2010;649(1-3):195–201.
27. Kang JY, Park SK, Guo TJ, et al. Reversal of trimethyltin-induced learning and memory deficits by 3, 5-dicaffeoylquinic acid. *Oxid Med Cell Longev*. 2016;2016.
28. Bryan NS, Grisham MB. Methods to detect nitric oxide and its metabolites in biological samples. *Free Radic Biol Med*. 2007;43(5):645–657.
29. Lu P, Mamiya T, Lu LL, et al. Silibinin prevents amyloid β peptide-induced memory impairment and oxidative stress in mice. *Br J Pharmacol*. 2009;157(7):1270–1277.
30. Uddin MS, Mamun AA, Hossain MS, Akter F, Iqbal MA, Asaduzzaman M. Exploring the effect of Phyllanthus emblica L. On cognitive performance, brain antioxidant markers and acetylcholinesterase activity in rats: promising natural gift for the mitigation of alzheimer's disease. *Ann Neurosci*. 2016;23(4):218–229.
31. Lowry O, Rosebrough N, Farr AL, Randall R. Protein measurement with the Folin phenol reagent. *J Biol Chem*. 1951;193(1):265–275.
32. Rahman SO, Panda BP, Parvez S, et al. Neuroprotective role of astaxanthin in hippocampal insulin resistance induced by Aβ peptides in animal model of Alzheimer's disease. *Biomed Pharmacother*. 2019;110:47–58.

33. Pradeepkiran JA, Reddy PH. Structure based design and molecular docking studies for phosphorylated tau inhibitors in alzheimer's disease. *Cells*. 2019;8(3):260.
34. Rajasekar N, Dwivedi S, Tota SK, et al. Neuroprotective effect of curcumin on okadaic acid induced memory impairment in mice. *Eur J Pharmacol*. 2013;715(1–3):381–394.
35. He J, Yamada K, Zou LB, Nabeshima T. Spatial memory deficit and neurodegeneration induced by the direct injection of okadaic acid into the hippocampus in rats. *J Neural Transm*. 2001;108(12):1435–1443.
36. Costa AP, Tramontina AC, Biasibetti R, et al. Neuroglial alterations in rats submitted to the okadaic acid-induced model of dementia. *Behav Brain Res*. 2012;226(2):420–427.
37. de Souza E Silva TG, do Val de Paulo MEF, da Silva JRM, et al. Oral treatment with royal jelly improves memory and presents neuroprotective effects on icv-STZ rat model of sporadic Alzheimer's disease. *Heliyon*. 2020;6(2), e03281.
38. Pyrzanowska J, Piechal A, Blecharz-Klin K, et al. Administration of Greek Royal Jelly produces fast response in neurotransmission of aged Wistar male rats. *J Pre Clin Res*. 2015;9(2):151–157.
39. Dashniani M, Chighladze M, Burjanadze M, Beselia G, Kruashvili L. Memantine attenuates the okadaic acid induced short-term spatial memory impairment and hippocampal cell loss in rats. *Georgian Med News*. 2016;(252):59–63.
40. Zhang H, Wang X, Xu P, et al. Tolfenamic acid inhibits GSK-3β and PP2A mediated tau hyperphosphorylation in Alzheimer's disease models. *J Physiol Sci*. 2020;70(1):29.
41. Hampel H, Mesulam MM, Cuello AC, et al. The cholinergic system in the pathophysiology and treatment of Alzheimer's disease. *Brain*. 2018;141(7):1917–1933.
42. Sims NR, Bowen DM, Allen SJ, et al. Presynaptic cholinergic dysfunction in patients with dementia. *J Neurochem*. 1983;40(2):503–509.
43. Kamat PK, Tota S, Rai S, et al. Okadaic acid induced neurotoxicity leads to central cholinergic dysfunction in rats. *Eur J Pharmacol*. 2012;690:90–98.
44. Kamat PK, Tota S, Shukla R, Ali S, Najmi AK, Nath C. Mitochondrial dysfunction: a crucial event in okadaic acid (ICV) induced memory impairment and apoptotic cell death in rat brain. *PharmacolBiochemBehav*. 2011;100(2):311–319.
45. Ishrat T, Parveen K, Khan MM, et al. Selenium prevents cognitive decline and oxidative damage in rat model of streptozotocin-induced experimental dementia of Alzheimer's type. *Brain Res*. 2009;1281:117–127.
46. Sastre M, Klockgether T, Heneka MT. Contribution of inflammatory processes to Alzheimer's disease: molecular mechanisms. *Int J Dev Neurosci*. 2006;24:167–176.
47. Rivers-Auty J, Mather AE, Peters R, Lawrence CB, Brough D. Alzheimer's Disease Neuroimaging Initiative, Anti-inflammatories in Alzheimer's disease—potential therapy or spurious correlate. *Brain Comm*. 2020;2(2):fcaa109.
48. Engmann O, Giese KP. Crosstalk between Cdk5 and GSK3beta: implications for alzheimer's disease. *Front Mol Neurosci*. 2009;2:2.
49. Sontag JM, Sontag E. Protein phosphatase 2A dysfunction in Alzheimer's disease. *Front Mol Neurosci*. 2014;7:16.
50. Yoon SY, Choi JE, Huh JW, Hwang O, Hong HN, Kim D. Inactivation of GSK-3beta in okadaic acid-induced neurodegeneration: relevance to Alzheimer's disease. *Neuroreport*. 2005;16:223–227.